NeuroImage 189 (2019) 214–223

Contents lists available at ScienceDirect

NeuroImage

journal homepage: www.elsevier.com/locate/neuroimage

# Individual variation in brain network topology is linked to emotional intelligence

George Ling [a,b,1], Ivy Lee [a,b,1], Synthia Guimond [a,b], Olivia Lutz [a,b], Neeraj Tandon [a,b], Uzma Nawaz [a,b], Dost Öngür [b,c], Shaun Eack [d], Kathryn E. Lewandowski [b,c], Matcheri Keshavan [a,b], Roscoe Brady Jr. [a,b,c,*]

[a] Department of Psychiatry, Beth Israel Deaconess Medical Center, Boston, MA, USA
[b] Department of Psychiatry, Harvard Medical School, Boston, MA, USA
[c] Schizophrenia and Bipolar Disorder Program, McLean Hospital, Belmont, MA, USA
[d] University of Pittsburgh, School of Social Work, Pittsburgh, PA, USA

ARTICLE INFO

*Keywords:*
Emotional intelligence
Magnetic resonance imaging
Social cognition
Schizophrenia
Network
Topography

ABSTRACT

*Background:* Social cognitive ability is a significant determinant of functional outcome, and deficits in social cognition are a disabling symptom of psychotic disorders. The neurobiological underpinnings of social cognition are not well understood, hampering our ability to ameliorate these deficits.
*Objective:* Using 'resting state' functional magnetic resonance imaging (rsfMRI) and a trans-diagnostic, data-driven analytic strategy, we sought to identify the brain network basis of emotional intelligence, a key domain of social cognition.
*Methods:* The study included 60 participants with a diagnosis of schizophrenia or schizoaffective disorder and 45 healthy controls. All participants underwent a rsfMRI scan. Emotional Intelligence was measured using the Mayer-Salovey-Caruso Emotional Intelligence Test (MSCEIT). A connectome-wide analysis examined how each individual brain voxel's connectivity correlated with emotional intelligence using multivariate distance matrix regression (MDMR).
*Results:* We identified a region in the left superior parietal lobule (SPL) where individual network topology is linked to emotional intelligence. Specifically, in high scoring individuals, this region is a node of the Default Mode Network and in low scoring individuals, it is a node of the Dorsal Attention Network. This relationship was observed in both schizophrenia and healthy comparison participants.
*Conclusion:* Prior studies have demonstrated individual variance in the topology of canonical resting state networks but the cognitive or behavioral relevance of these differences has largely been undetermined. We observe that the left SPL, a region of high individual variance at the cytoarchitectonic level, also demonstrates individual variance in its association with large scale resting-state networks and that network topology is linked to emotional intelligence.

## 1. Introduction

Social cognition is a multidimensional construct encompassing a number of mental processes related to perception of, interpretation of, and response to the social environment (Green et al., 2008). These processes include: inferring the mental state of others, correctly interpreting social cues, understanding social context, and emotional intelligence. Deficits in multiple domains of social cognition are well-described in patients with psychotic disorders (Bora et al., 2009; Dodell-Feder et al., 2014; Green et al., 2015; Kohler et al., 2010; Mehta et al., 2014; Savla et al., 2013; Sprong et al., 2007). These deficits may be both partially independent of neurocognitive deficits and strongly associated with functional status (Allen et al., 2007; Fett et al., 2011; Green, 2016; Hoe et al., 2012; Mehta et al., 2013; Sergi et al., 2007). These findings suggest that social cognitive functioning may be underpinned by neurobiological processes that are at least partially distinct from those associated with

* Corresponding author. Massachusetts Mental Health Center, 75 Fenwood Road Room 616, Boston, MA, 02115, USA.
*E-mail address:* robrady@bidmc.harvard.edu (R. Brady).
[1] These authors contributed equally to this manuscript.

https://doi.org/10.1016/j.neuroimage.2019.01.013
Received 23 July 2018; Received in revised form 26 October 2018; Accepted 6 January 2019
Available online 8 January 2019

other cognitive processes and contribute uniquely to poor functional outcomes in schizophrenia.

Studies of the neuroanatomical basis of social cognitive ability have frequently utilized functional magnetic resonance imaging (fMRI) in both clinical and non-clinical populations to identify brain regions associated with various domains of social processing (see (Green et al., 2015) for review). Recent studies examining task-free 'resting state' brain connectivity have found abnormal functional connectivity in medial prefrontal and temporal networks that are correlated with social cognitive dysfunction (Abram et al., 2017). Functional connectivity in these areas, commonly associated with the default mode network (DMN), has been linked to social cognition and real world social functioning in participants with schizophrenia, first-degree relatives of people with schizophrenia, and healthy comparison participants (Dodell-Feder et al., 2014; Fox et al., 2017).

Among the diverse processes encompassed by social cognition, a critical domain is emotional intelligence, "the subset of social intelligence that involves the ability to monitor one's own and others' feelings and emotions, to discriminate among them and to use this information to guide one's thinking and actions" (Salovey and Mayer, 1990). Emotional intelligence is commonly measured using the Mayer-Salovey-Caruso Emotional Intelligence Test (MSCEIT) (Mayer et al., 2003). This test reliably detects social cognitive deficits and is a predictor of social functioning (Eack et al., 2010; Nuechterlein et al., 2008). Performance on the different subscales of this test are highly correlated and for this reason, the 'managing emotions' subscale of the MSCEIT was chosen as the sole measure of social cognition in the battery of tests recommended by the National Institutes of Mental Health Measurement and Treatment Research to Improve Cognition in Schizophrenia (MATRICS) (Marder, 2006). The broad adoption of the MATRICS Consensus Cognitive Battery (MCCB) by cognition researchers allows standardized and validated testing of emotional intelligence across different sites and research groups.

In this study we sought to identify the brain network correlates of emotional intelligence. We made three methodological decisions in our approach:

First, published hypothesis-driven approaches have been constrained in their ability to capture findings outside the experimental model. We therefore chose to conduct a connectome-wide, entirely data-driven approach to elucidate relationships between social cognition and connectivity.

Second, deficits in social cognitive ability are related to functional outcome in both clinical and non-clinical populations (Dodell-Feder et al., 2014). We sought to discover common dimensional relationships between cognition and connectivity. We hypothesized that the combination of a connectome-wide data analysis with a study sample of schizophrenia and healthy comparison participants would demonstrate trans-diagnostic relationships between connectivity and cognition.

Third, we measured emotional intelligence using the MSCEIT subscale included in the MCCB because this allowed us to combine data from multiple sites and studies to identify robust and replicable correlations between connectivity and intelligence.

We determined the relationship between emotional intelligence and functional connectivity at the level of individual brain voxels using multivariate distance matrix regression (MDMR), a technique for connectome-wide association studies (Shehzad et al., 2014). We examined this correlation in a group of over one hundred participants recruited across three distinct sites including individuals with schizophrenia or schizoaffective disorder as well as healthy comparison participants.

We hypothesized that this approach would identify brain networks that mediate emotional intelligence trans-diagnostically. Given the existing literature (cited above) implicating the medial prefrontal and temporal cortices, we predicted that network hubs of the DMN in these regions would be included in our findings.

## 2. Material and methods

### 2.1. Participants

The study was approved by the Institutional Review Boards of the University of Pittsburgh (Pittsburgh, PA), McLean Hospital (Belmont, MA), and Beth-Israel Deaconess Medical Center (Boston, MA), and all participants gave written informed consent before participating. Participants were recruited from health centers using a variety of means including early psychosis treatment programs and community referral networks. Participants at the Boston and Pittsburgh sites were recruited for a clinical trial (BICEPS, NCT01561859). Clinical and imaging data analyzed here was from participants' baseline (pre-intervention) evaluation.

Diagnosis was determined using the Structured Clinical Interview for the DSM-IV (SCID) (First and New York State Psychiatric Institute. Biometrics Research, 2007). Patients were assessed by raters trained in the administration and scoring of the SCID. Inclusion criteria for all participants included: (1) age 18–45 years; (2) current IQ $\geq$ 80 as assessed using the WASI-II (Hays et al., 2002); and (3) the ability to read (sixth grade level or higher) and speak fluent English. Additional inclusion criteria for psychotic disorder participants were (1) a diagnosis of schizophrenia or schizoaffective disorder verified using the SCID interview (First, 1998); (2) time since first psychotic symptom of $\leq$8 years; and (3) clinically stabilized on antipsychotic medication (assessed via SCID in consensus conferences). Healthy comparison (HC) participants did not meet criteria for any Axis I psychiatric disorder currently or historically.

Exclusion criteria were (1) significant neurological or medical disorders that may produce cognitive impairment (e.g., seizure disorder, traumatic brain injury); (2) persistent suicidal or homicidal behavior; (3) a recent history of substance abuse or dependence (within the past 3 months); (4) any MRI contraindications and (5) decisional incapacity requiring a guardian.

Demographic, clinical, and medication regimen information are summarized in Supplemental Table 1.

### 2.2. Cognitive testing

Participant emotional intelligence was assessed using the MATRICS Consensus Cognitive Battery (MCCB) (Nuechterlein et al., 2008). This testing battery includes 7 composite scores of processing speed, attention, working memory, verbal learning, visual learning, problem solving, and social cognition. The social cognition score is calculated from the Mayer-Salovey-Caruso Emotional Intelligence Test (MSCEIT) "managing emotions" subscale (Mayer et al., 2003). The MSCEIT includes a series of vignettes. Participants are presented with a series of possible actions related to each vignette and asked to assess the effects of each action on the actor's or other characters' mood states or behaviors. Responses are based on a Likert-type scale. We used age and sex normed T scores, which were calculated using the MCCB scoring package.

### 2.3. MRI data acquisition

#### 2.3.1. Boston & Belmont sites

Data were acquired on 3T Siemens Trio (TIM upgrade) scanners using a standard head coil. The echoplanar imaging parameters were as follows: repetition time, 3000 ms; echo time, 30 ms; flip angle, 85°; 3 × 3 × 3-mm voxels; and 47 axial sections collected with interleaved acquisition and no gap. Structural data included a high-resolution T1 image. In addition, all participants underwent a resting fMRI run with the instructions 'remain still, stay awake, and keep your eyes open'. Each functional run lasted 6.2 min (124 time points).

#### 2.3.2. Pittsburgh site

Data were acquired on a 3T Siemens Verio scanner using a standard head coil. The echoplanar imaging parameters were as follows: repetition

time, 3000 ms; echo time, 30 ms; flip angle, 85°; 3 × 3 × 3-mm voxels; and 45 axial sections collected with interleaved acquisition and no gap. Structural data included a high-resolution T1 image. In addition, all participants underwent a resting fMRI run that lasted 6.2 min (124 time points).

### 2.4. MRI data processing

The imaging data was preprocessed using DPABI image processing software (Yan et al., 2016). To minimize effects of scanner signal stabilization, the first four images were omitted from all analysis. Scans with head motion exceeding 3 mm or 3° of maximum rotation through the resting-state run were discarded (n = 28). Functional and structural images were co-registered. Structural images were then normalized and segmented into gray, white and CSF partitions using the DARTEL technique (Ashburner, 2007). A Friston 24-parameter model (Friston et al., 1996) was used to regress out head motion effects from the realigned data. CSF and white matter signals, global signal as well as the linear trend were also regressed out. The decision to regress the global signal was based on prior demonstration that the combination of this step plus volume-wise 'scrubbing' for head 'micromovements' is an effective strategy for removal of motion artifacts (Yan et al., 2013). After realigning, slice timing correction, and co-registration, framewise displacement (FD) was calculated for all resting state volumes (Power et al., 2012). All volumes within a scan with a FD greater than 0.2-mm were censored. Any scan with at least 50% of volumes requiring censoring was discarded (n = 18). After nuisance covariate regression, the resultant data were band-pass filtered to select low frequency (0.01–0.08 Hz) signals. Filtered data were normalized by DARTEL into MNI space and then smoothed by a Gaussian kernel of 8 $mm^3$ full-width at half maximum (FWHM). Voxels within a group derived gray matter mask were used for further analyses.

After preprocessing, a total of 60 participants with schizophrenia or schizoaffective disorder, and 45 HC participants across all sites remained in the study (Supplemental Table 1).

### 2.5. Functional connectivity analysis

#### 2.5.1. Multivariate distance matrix regression

We performed a connectome-wide association study using multivariate distance matrix regression (MDMR) as originally described in (Shehzad et al., 2014). Briefly, MDMR tests every voxel to determine if whole-brain connectivity to that voxel is more similar in individuals with similar MSCEIT score than in individuals with dissimilar MSCEIT score. As previously described (Satterthwaite et al., 2015; Shanmugan et al., 2016; Sharma et al., 2017), this analysis occurs in several stages: First, a seed-to-voxel connectivity map is generated by using an individual voxel's BOLD signal time-course to calculate the temporal Pearson's

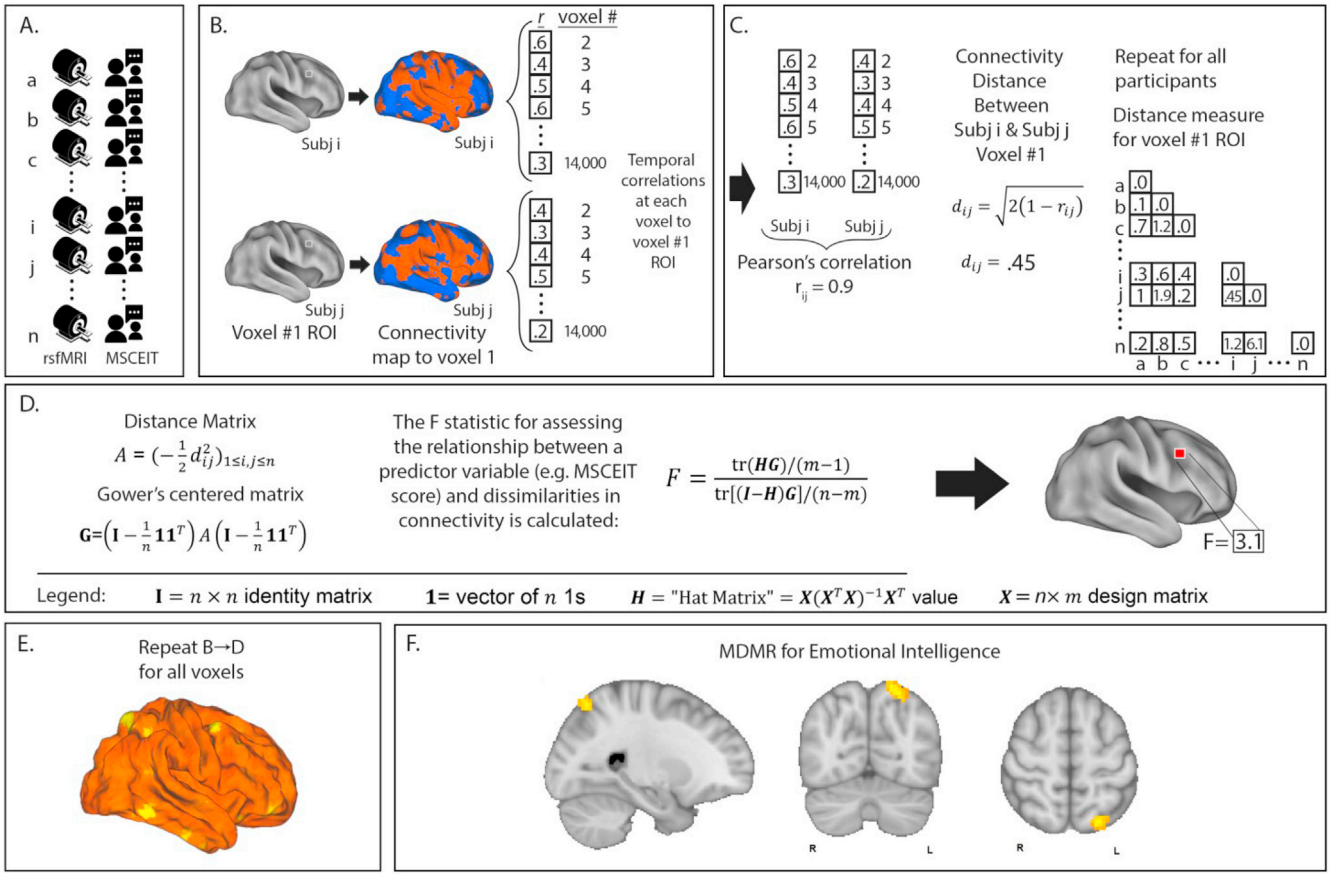


**Fig. 1.** Multivariate Distance Matrix Regression identifies brain voxels whose functional connectivity varies with performance on a measure of emotional intelligence. MDMR procedure: A. rsfMRI and emotional intelligence testing are collected from each participant. B. For each participant a functional connectivity map is generated to an individual voxel. C. Voxelwise temporal correlations between participants are used to generate a Pearson's correlation r and a distance metric d. This is repeated for all participants to generate a matrix of between subject distances. D. The distance matrix is centered and an ANOVA-like test is used to generate an F-statistic to assess the relationship between a predictor variable (MSCEIT score) and dissimilarities in functional connectivity at that voxel. E. This process is repeated for every voxel. This results in a whole brain map of how significantly functional connectivity is related to emotional intelligence. Permutation testing then identifies whole-brain significant clusters in connectivity-MSCEIT relationships. F. In our sample of 105 participants (n = 60 with schizophrenia or schizoaffective disorder and n = 45 HC participants), we identified a single region in the left superior parietal lobule (extent k = 59, centered at MNI coordinates X-24 y-69 z+57) whose connectivity correlated significantly with emotional intelligence. In this image, connectivity is thresholded at a voxelwise level of p < .001 and extent threshold of p < .05.

correlation coefficients between that voxel and all other gray matter voxels(Fig. 1B). These maps are generated for every participant. In the second stage, the temporal correlation coefficients for each voxel in the connectivity map is correlated with the values of corresponding voxels in maps generated from every other participant. This Pearson's correlation coefficient, $r$ is a measure of the similarity of whole-brain connectivity to that voxel between patients. This value is used to calculate between-subject distance (or dissimilarity) using the metric $d_{ij} = \sqrt{2(1-r_{ij})}$ where $i$ and $j$ are two subjects and $r$ is the correlation coefficient above. (Fig. 1C)(Zapala and Schork, 2006). The next stage tests the relationship between a given variable (here MSCEIT score) and the inter-subject distances in connectivity generated in the previous stage. Broadly speaking, this process consists of ANOVA-like hypothesis testing where the tested relationship is between a variable of interest and a matrix of distances. This process was originally termed multivariate distance matrix regression by Zapala and Schork and used to test associations between gene expression and related variables (Zapala and Schork, 2006). Shezhad et al. then used their framework for testing the relationship between variables of interest and a matrix of distances where the matrix is between-subject similarity in whole-brain functional connectivity. This test consists of first forming a distance matrix $A = \left(-\frac{1}{2}d_{ij}^2\right)_{1\le i,j\le n}$ among $n$ participants where $d =$ the between subject distance metric calculated above. Next, this matrix is used to create a Gower's centered matrix.

$\mathbf{G} = \left(\mathbf{I} - \frac{1}{n}11^T\right)A\left(\mathbf{I} - \frac{1}{n}11^T\right)$, in which $n$ is the number of participants, $\mathbf{I}$ is the $n \times n$ identity matrix, and 1 is a vector of $n$ 1s. The $F$ statistic for assessing the relationship between a predictor variable (e.g. MSCEIT score) and dissimilarities in connectivity is calculated as follows: For $m$ predictor variables, let $\boldsymbol{X}$ be a $n \times m$ design matrix of predictor values, and let $\boldsymbol{H} = \boldsymbol{X}(\boldsymbol{X}^T\boldsymbol{X})^{-1}\boldsymbol{X}^T$ be the associated $n \times m$ "hat" matrix.

$F = \frac{\mathrm{tr}(\boldsymbol{HG})/(m-1)}{\mathrm{tr}[(\boldsymbol{I}-\boldsymbol{H})\boldsymbol{G}]/(n-m)}$ (Fig. 1D) (Shehzad et al., 2014). This process is repeated for every voxel. The result is a whole brain map of how significantly MSCEIT scores are related to functional connectivity at every voxel (Fig. 1E). From that map, ROIs for follow-up analysis are defined based on clusters of significant voxelwise F-statistics. To correct for multiple comparisons, a nonparametric permutation was calculated for voxels that exceeded the significance threshold of $p < .001$ and clusters of such with an extent threshold of $p < .05$, with a null distribution calculated from 5000 such permutations (Fig. 1F). Scanner site was included as a covariate in this analysis. The voxelwise threshold was selected to maximize the likelihood of replicability.

This analysis identifies anatomical regions where MSCEIT score is significantly related to functional connectivity. Recall that at each brain voxel MDMR calculates a distance metric $r$ between subjects by first calculating the temporal correlation in BOLD signal between that voxel and every other brain voxel. The generated set of temporal correlations is then correlated with the analogous set of temporal correlations from a different subject. The resulting between-subject correlation determines a distance metric that is a measure of between-subject similarity (or dissimilarity) in terms of functional connectivity at that voxel. Notably, this process disregards spatial information about the voxels that gave rise to between-individual distances e.g. Two individuals may be very distant (dissimilar) in the functional connectivity of a voxel in the precuneus, but is their dissimilarity driven by differences in precuneus connectivity to the mPFC or temporal lobe or parietal lobe or all of the above? MDMR as implemented by Shehzad et al. does not display this information (Shehzad et al., 2014). To visualize this spatial information requires follow-on seed-based connectivity analysis. Shehzad et al. and others have termed this follow-on analysis 'post-hoc' testing to make clear that this should not be considered independent hypothesis testing nor should it be considered independent validation of the original MDMR finding (Satterthwaite et al., 2015; Shanmugan et al., 2016; Sharma et al., 2017; Shehzad et al., 2014). As in these prior manuscripts, we conducted the MDMR analysis to find anatomical regions where connectivity significantly varied with MSCEIT score and then conducted follow-on seed--based connectivity analysis to examine the spatial distribution of these connectivity differences.

#### 2.5.2. Seed based connectivity analyses

For seed based connectivity analyses we used DPABI to extract the time course of the BOLD signal in a given ROI. We then generated whole brain maps of z-transformed Pearson's correlation coefficients. These maps were entered into SPM12 (Statistical and Parametric Mapping, http://www.fil.ion.ucl.ac.uk/spm). For ROIs generated from MDMR above, we regressed the maps against MSCEIT score to generate spatial maps of how whole brain functional connectivity to the ROIs varies with MSCEIT score. To control for participant variables of non-interest, we performed these analyses with age, race, diagnosis (Schizophrenia or Healthy Comparison), scanner site, and sex as additional covariates. To control for movement effects we also included individual mean FD (framewise displacement) as a covariate as a subject-level correction for motion effects in all subjects (Power et al., 2012). In addition to including mean FD as a covariate in the seed-based connectivity analysis, we did not observe a significant correlation between MSCEIT score and either mean within-scanner movement as measured by average framewise displacement ($r = -0.109$, $p = .268$), nor did we observe a significant correlation between MSCEIT score and the number of volumes remaining after preprocessing for movement ($r = 0.14$ and $p = .15$).

To control for the effects of medication regimen, the analyses were re-performed with prescribed anti-psychotic dosage (in chlorpromazine equivalents, CPZE) as a covariate within the schizophrenia/schizoaffective group.

For other, subsequent ROI based connectivity analyses described below, we used DPABI to calculate the time course of the average BOLD signal in a sphere, and then generated whole brain maps of z-transformed Pearson's correlation coefficients. We then used SPM12 to generate single-sample t-tests of these connectivity maps.

#### 2.5.3. Correlations between ROI to ROI connectivity and emotional intelligence

Partial correlation coefficients and statistic values were calculated in R using the *ppcor* package(Kim, 2015). *N*th-order partial correlation coefficients are Pearson's correlations between two variables of interest while controlling for $n$ covariates. Categorical covariates were binarized.

### 2.6. Structural MRI analysis

Structural MPRAGE images were checked for artifacts and were processed using Freesurfer 6 (http://surfer.nmr.mgh.harvard.edu/). The images went through first-level auto-reconstruction to register the scans in standard space and skull strip the brains. One rater (OL) edited the images to remove dura, sinuses and vessels that could interfere with segmentation. After visual inspection, 98 images were retained for analysis. The images then went through second and third level auto-reconstruction to register the brains to the Desikan-Killiany atlas and extract sulcal depth measurements (Desikan et al., 2006). Sulcal depth in Freesurfer is the integrated dot product of the movement vector and the surface normal during inflation. Deep regions therefore are expressed as positive values as they move outwards while more superficial regions move inwards. Units are the standard deviation from the median value.

### 2.7. Table and figure generation

Graphs of relationships between emotional intelligence and structural/functional measures were generated using R. Projections of ROIs and T contrast maps onto cortical surfaces was accomplished using FSL (Jenkinson et al., 2012), Caret (Van Essen et al., 2001) and Surf Ice (www.nitrc.org/projects/surfice/).

## 3. Results

### 3.1. Functional connectivity in the superior parietal lobule is linked to emotional intelligence

MDMR analysis performed across all 105 participants (60 schizophrenia, 45 HC) revealed a single region whose intrinsic functional connectivity correlated significantly with emotional intelligence. This identified a (59 voxel) region in the left superior parietal lobule (SPL) centered at MNI coordinates X-24 y-69 z+57 (Fig. 1F).

### 3.2. SPL association with distributed brain networks is linked to emotional intelligence

We performed follow-on analysis using this SPL region in a seed-based connectivity analysis to determine the spatial distribution and directionality of connectivity that gave rise to this result. This analysis revealed two apparent patterns of functional connectivity: higher emotional intelligence correlated with increasing intrinsic connectivity between the left SPL and bilateral fronto-parietal and temporal regions that correspond to the canonical "default mode network" (DMN) (Fig. 2A). Inversely, lower emotional intelligence correlated with increasing functional connectivity between the left SPL and bilateral parietal-occipital regions that mirror the canonical distribution of the "dorsal attention network" (DAN) (Fig. 2B).

To confirm the identity of these apparent emotional intelligence – network connectivity relationships, we compared our observed whole brain correlations to existing, independently determined maps of the DMN and DAN (Yeo et al., 2011). We observed clear overlap between the networks identified here and the DMN and DAN (Supplemental Fig. 1).

We plotted the relationship between emotional intelligence and functional connectivity for both networks as a scatter plot in Fig. 2C and D. As expected from the maps in Fig. 2A and B, we observed that higher emotional intelligence was correlated with increased functional connectivity between the SPL and the DMN and decreased connectivity to the DAN. Because the DMN is intrinsically anti-correlated with the DAN, this result could be expected for any region in one of these networks (i.e. a region of interest located in the distribution of the DMN that demonstrated lower correlation to the rest of the DMN would be expected to demonstrate higher correlation to the DAN). Surprisingly, the scatter plots of connectivity cross the axis of 0 connectivity i.e. *activity in this SPL region is intrinsically correlated to the DMN in some individuals and is intrinsically correlated to the DAN in others.*

### 3.3. Connectivity associations with emotional intelligence controlling for diagnosis and medication regimen

The observed connectivity-intelligence relationships were highly significant even when controlled for diagnosis (schizophrenia vs healthy control). We examined the strength of functional connectivity – emotional intelligence relationships in HC participants and those with schizophrenia/schizoaffective disorder independently. Using the same ROIs as in Fig. 2C and D, we correlated FC with emotional intelligence. We observe similar strengths of correlation between emotional intelligence and DMN-SPL connectivity in HC ($r = 0.45$, $p = .004$) and schizophrenia ($r = 0.59$, $p < .001$) samples. We also see similar correlation strengths in DAN-SPL connectivity in HC ($r = -0.48$, $p = .002$) and schizophrenia samples ($r = -0.69$ $p < .001$) (Supplemental Fig. 2A). To control for the effects of prescribed antipsychotic regimen (within the schizophrenia/schizoaffective group), we reexamined SPL to network connectivity with this variable regressed out as a covariate. We continued to observe the same significant emotional intelligence – network connectivity relationships even when controlling for this and other confounding variables simultaneously (Supplemental Figs. 2A and B).

### 3.4. Domain specificity of SPL connectivity-cognition relationships

As an exploratory analysis, we asked whether the network connectivity of the SPL region correlated to cognitive ability broadly or was specific to emotional intelligence. We examined connectivity to this ROI regressed against MSCEIT score with full scale IQ (FSIQ) as a covariate. This was performed on participants in the study with FSIQ data available (BICEPS i.e. Pittsburgh and Boston). In this analysis, we again observed the same pattern of emotional intelligence correlated functional connectivity as seen without FSIQ as a covariate (Supplemental Fig. 3).

### 3.5. Site replicability of connectivity-cognition relationships

Given significant concerns about the replicability of fMRI imaging studies, we sought to determine if these findings in the total sample could be observed in each study population (BICEPS and McLean Hospital) independently to better confirm the replicability of this result. Both study populations independently observe the same pattern of SPL functional connectivity correlating with emotional intelligence (i.e. DMN connectivity with higher emotional intelligence and DAN connectivity with lower emotional intelligence) (Supplemental Fig. 4).

### 3.6. Emotional intelligence is linked to brain network topology

The implication of the results presented in Fig. 2C and D is that in the highest performing participants, activity in this SPL region is intrinsically correlated to the DMN, while in the lowest performing participants, this region is intrinsically correlated to the DAN. The identified networks display a clear correspondence to the canonical distribution of the DMN and DAN (Supplemental Fig. 1). To avoid circularity in defining these networks, we sought to validate the identity of these networks using methods that are not intrinsic to this study. We used one of the original methods for identifying the DMN and DAN, measuring connectivity to ROIs in the precuneus (DMN) and frontal eye fields (DAN) (Fox et al., 2005). We then compared the topology of these networks in all study participants. As expected from the results in Fig. 2, we observe that, the relationship between network topology and emotional intelligence is continuous for individuals (Fig. 3).

### 3.7. Sulcal depth associations with emotional intelligence

Prior studies have revealed considerable individual variation at the cytoarchitectonic level in this region (see discussion). That level of analysis is not available in the current data, but we asked whether there is a structural MRI correlate to network connectivity and emotional intelligence in this region. We hypothesized that emotional intelligence would be correlated with sulcal depth in this region based on two prior studies of this region: First, Mueller et al. noted high individual variability in sulcal depth but not cortical thickness in this region (Mueller et al., 2013). Second, Wang et al. demonstrated that the intra-parietal sulcus area hIP3 may be associated with a DMN-like pattern of connectivity (Wang et al., 2015b). We hypothesized that greater sulcal depth would be correlated with both greater functional connectivity to the DMN as well as higher emotional intelligence scores. As predicted, we observed a significant ($r = 0.269$, $p = .0075$) relationship between sulcal depth and emotional intelligence (Fig. 4).

## 4. Discussion

We identified a region of the left superior parietal lobule whose intrinsic functionally connectivity correlates significantly with emotional intelligence. Surprisingly, the relationship between connectivity and cognition appears to be mediated by individual variation in the topological distribution of two large scale resting-state brain networks, the DMN and the DAN. The brain is organized into distributed resting-state networks whose topology are typically visualized using group

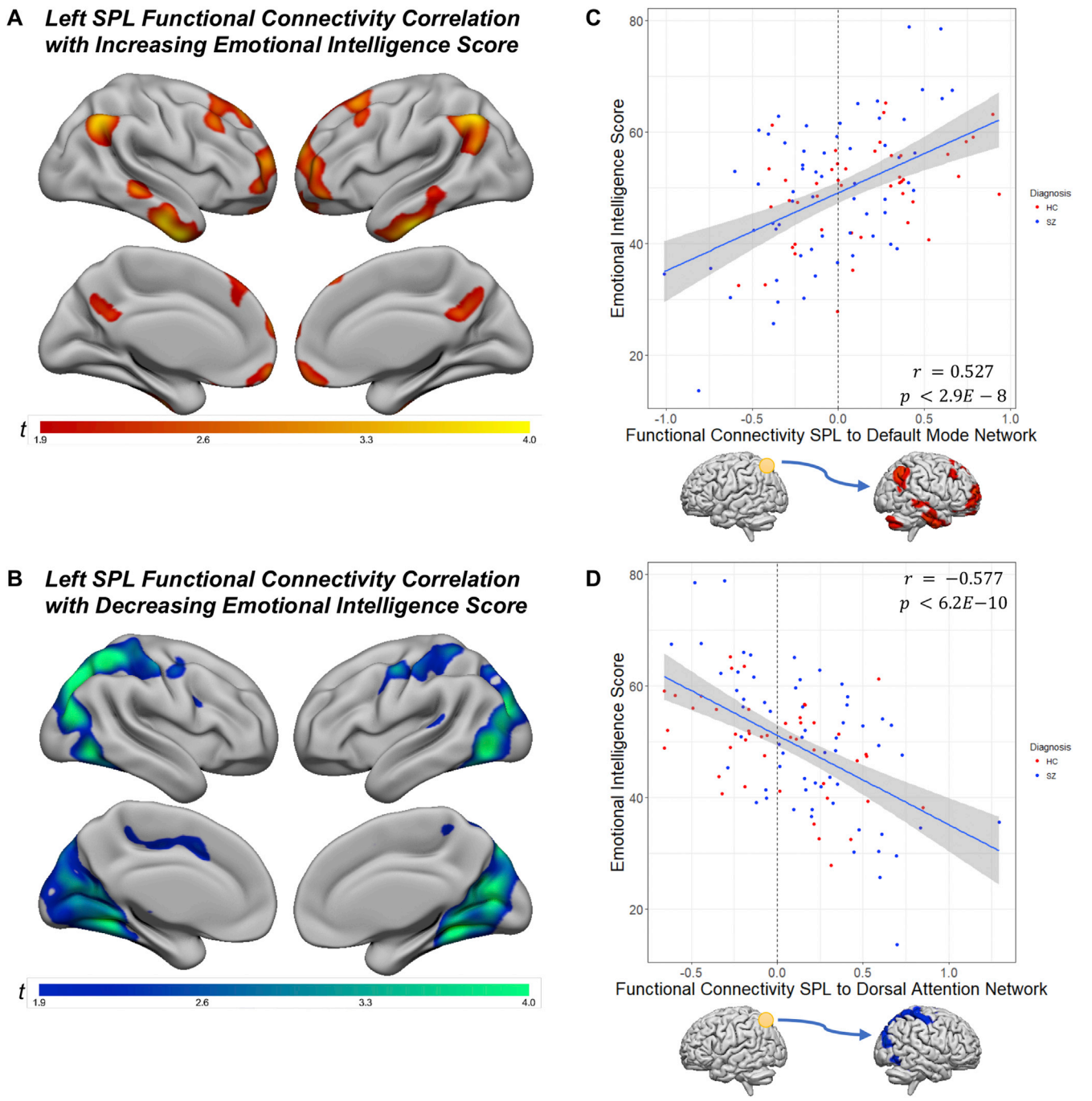


**Fig. 2.** Emotional Intelligence is Linked to Network Topography.
Follow-on analysis to determine the spatial pattern and directionality of connectivity that gave rise to the MDMR result. Two patterns of connectivity are observed. A. Emotional intelligence is correlated with functional connectivity between the left SPL region and the "default mode network" (DMN). B. Emotional intelligence is inversely correlated with functional connectivity between the left SPL and the "dorsal attention network" (DAN). Color bar: t-statistic > 1.9 (97.5% threshold). C. Plot of emotional intelligence score (y-axis) and functional connectivity between 6 mm sphere at SPL ROI coordinates (X-24 y-69 z+57) and the DMN network shown in 2A (x-axis). D. Plot of emotional intelligence (y-axis) and functional connectivity between 6 mm sphere at SPL ROI coordinates X-24 y-69 z+57 and the DAN network shown in 2B (x-axis). Notably, both graphs demonstrate correlations that cross the reference line of null functional connectivity, meaning that this ROI does not simply display cognition-connectivity correlations within the DMN and expected cognition-connectivity anti-correlations in the network (DAN) anti-correlated with the DMN. Rather, the network association of this region appears to shift from being a member of the DMN to a member of the DAN as one moves along the distribution from higher scoring individuals to lower scoring individuals.

averaging (Power et al., 2011; Yeo et al., 2011). Individual variation in network topology among healthy control participants has been demonstrated previously (Gordon et al., 2017a, 2017b; Laumann et al., 2015; Mueller et al., 2013; Poldrack et al., 2015; Wang et al., 2015a). A separate field of inquiry has identified functional connectivity correlates of cognitive abilities such as sustained attention (Rosenberg et al., 2016), fluid intelligence (Finn et al., 2015) and a variety of behavioral traits (Smith et al., 2015). Until recently, the contribution of individual network topology to cognitive variation has been undetermined but a recent report has linked DMN topology to several cognitive and behavioral phenotypes (Bijsterbosch et al., 2018). Here we demonstrate that emotional intelligence is linked to the topology of two canonical

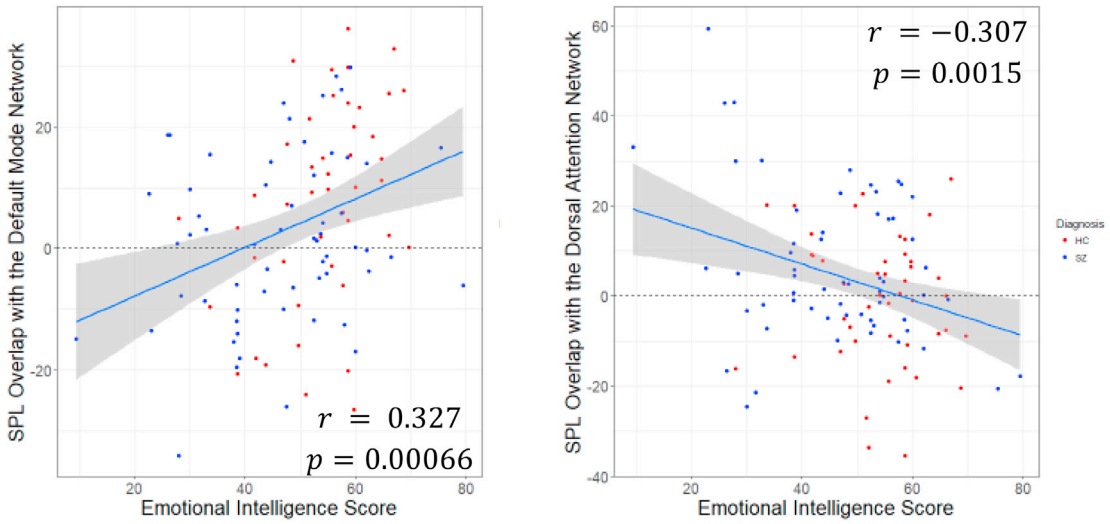


**Fig. 3.** Validation of the relationship between emotional intelligence and network topography.
Although the spatial distribution of connectivity in Fig. 2A and B matched the distribution of the DMN and DAN respectively, we sought to test intelligence-network connectivity relationships using methods extrinsic to the study. The topographic distribution of the Default Mode Network and Dorsal Attention Network are visualized using canonical methods: The topographic distribution of the DMN is derived from functional connectivity to a 10-mm spherical ROI placed in the precuneus (x-4, y-58, z+44) and the DAN from a 10-mm sphere ROI placed in the frontal eye fields (x28 y-8, z+52). The overlap in individual canonically-derived topographic distribution and the L-SPL is explored in the total sample as a function of summed z-transformed functional connectivity scores between the L-SPL ROI and the above canonical nodes of the DMN and DAN. The same relationships between emotional intelligence and membership in the DMN (r = 0.327, p = .00066) and the DAN (r = −0.307, p = .0015) are observed using this approach.

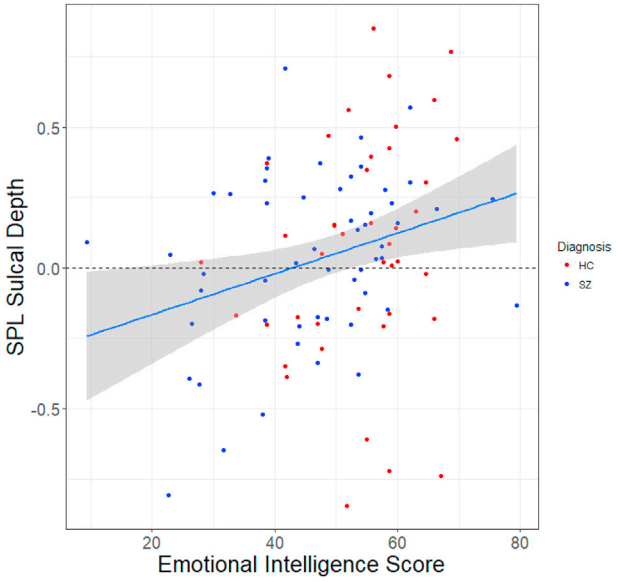


**Fig. 4.** Emotional intelligence is correlated with sulcal depth in the left SPL.
The Freesurfer program was used to calculate sulcal depth in the left superior parietal lobule ROI from the Desikan-Killiany atlas (the only ROI in the atlas that overlapped with the MDMR identified region). These values were then correlated with emotional intelligence scores with site as a covariate. Units are standard deviations from the median. This analysis revealed a significant correlation between sulcal depth and emotional intelligence (r = 0.269, p = .0075).

resting-state networks in a critical SPL region: in high performers, spontaneous activity in this region is correlated with the default mode network and in low performers this region is correlated with the dorsal attention network.

What is the basis of this variability in network membership of the SPL? A convergence of results from multiple research methods have demonstrated that the SPL can be subdivided into at least four distinct subregions that are differentiable on the basis of cytoarchitectonic description (Scheperjans et al., 2008), white matter tractography (Mars et al., 2011), and both task evoked and resting state functional connectivity (Wang et al., 2015b). Particularly relevant to this study is the finding that postmortem cytoarchitectonic studies identified considerable individual heterogeneity in the SPL (Scheperjans et al., 2008). The topographical distribution of these subregions in the left SPL was observed to show significant inter-subject variability, particularly in the region referred to as area 7A whose center of gravity corresponds to the region identified in this study.

Using group-averaged functional connectivity maps of the SPL, Wang et al. observed specific patterns of resting state connectivity to left SPL subregions (Wang et al., 2015b). That study identified five different "clusters" of resting state connectivity to the left SPL. Notably, the adjacent "L3 and L4" regions in that manuscript demonstrate specific connectivity patterns similar to the DMN and DAN patterns we observe among emotional intelligence high and low performers respectively. These regions appear to correspond to the hIP3 & 7A regions respectively, identified by Scheperjans et al. (2008). Moving outside of these regions, when we examine connectivity at coordinates that correspond to the other SPL subdivisions i.e. the Scheperjans 5L/Wang L2 region rostral to the MDMR ROI or the Scheperjans 7P/Wang L5 caudal to the MDMR ROI, we do not see a correlation between connectivity and emotional intelligence (Supplemental Materials text and Supplemental Fig. 5).

We hypothesize that the individual variability in resting state connectivity in this ROI identified by MDMR represents individual variability in the cytoarchitectonic organization of the left SPL. Furthermore, we hypothesize that the correlation between network connectivity and emotional intelligence is a cognitive correlate of this anatomic variability. To date, studies have not linked cytoarchitectonic variation in the SPL to cognitive variation. In support of this hypothesis, one existing study has correlated diffusion tensor imaging measures with performance on the same emotional intelligence test used in this study. In that article, Pisner et al. observed emotional intelligence correlating with increased fractional anisotropy in the cingulum connecting frontal and parietal regions in a distribution entirely consistent with our observation of emotional intelligence correlating with fronto-parietal connectivity (Pisner et al., 2017).

There is converging evidence suggesting that the DMN has a

particular role in social cognition (Dodell-Feder et al., 2014; Fox et al., 2017; Mars et al., 2012). The DMN is a large, distributed brain network. Why does such a circumscribed region of this network in the superior parietal lobule appear to be such a critical determinant of emotional intelligence? A neuroanatomical model called the parieto-frontal integration theory (P-FIT) suggests that connectivity between parietal cortex and frontal areas is a critical determinant of intelligence (Jung and Haier, 2007). In this specific scenario, connectivity between the parietal lobule and a parieto-frontal network implicated in social cognition (the DMN) may mediate emotional intelligence.

We hypothesize that the results of this study are convergent with prior work implicating a continuum of DMN connectivity and a broad spectrum of lifestyle choices that span a spectrum of adaptive and maladaptive behaviors (Smith et al., 2015). Bijsterbosch et al. recently demonstrated that in the Human Connectome Project (HCP) dataset, increasingly 'positive' or adaptive behaviors were associated with DMN topology that included more dorsal regions of the parietal lobe (Bijsterbosch et al., 2018). We believe that some of the behavioral associations identified in that work are linked with social cognitive ability and that despite using different imaging methods, different cognitive/behavioral metrics, and an independent sample of participants, we are observing a singular biological process.

In our study, the relationship between SPL network membership and emotional intelligence was trans-diagnostic and is observed in both participants with schizophrenia and schizoaffective disorder as well as HC participants. This is observed despite a representative patient sample in which the mean emotional intelligence score was significantly less than that of HC participants ($p = .015$). We hypothesize that what is already known about schizophrenia network pathophysiology may explain social cognition deficits in this disorder. There is evidence that the molecular pathophysiology believed to underlie schizophrenia leads to the selective disruption of fronto-parietal networks (e.g. the DMN) that is a hallmark feature of schizophrenia and related disorders (Baker et al., 2014; Yang et al., 2016). If social cognitive ability is partially dependent on left SPL connectivity to an intact DMN, our result may provide a mechanistic bridge linking a "synaptic" disease to poor societal functioning.

Limitations of this study include the fact that MSCEIT "managing emotions" subscale is only one of several measures of emotional intelligence. We have chosen to focus on this specific measure because this specific test (and not the other MSCEIT subscales) is included in the MATRICS Consensus Cognitive Battery (MCCB). The MCCB has achieved widespread use and this fact both allowed us to combine independently collected datasets (i.e. McLean data that collected this subscale as part of the MCCB with BICEPS data that collected this subscale as part of the full MSCEIT test). Notably, performance on the four subtests of the MSCEIT are well described by a single factor solution. Another limitation with our study and other cohort imaging studies is that this study is inherently correlational and cannot distinguish between connectivity directly causing cognitive performance versus other interpretations, e.g. the result of an underlying process that mediates social cognitive ability and network connectivity via unrelated processes.

Ultimately, interventions designed to improve emotional intelligence that incorporate imaging will validate or refute this network-based model of emotional intelligence by measuring network connectivity longitudinally before and after interventions to improve performance. This may be particularly relevant for behavioral clinical trials that utilize a "target engagement" framework to validate experimental therapeutics (Lewandowski et al., 2017). In that vein, the location of our result provides a potential target for neuromodulation. For example, If the network "membership" of this region can be modified via induction of neuroplasticity at this region (e.g. by repetitive transcranial magnetic stimulation), then neuromodulation may enhance trials using cognitive remediation interventions.

## 5. Conclusions

Prior studies have demonstrated individual variance in the topology of canonical resting state networks but the cognitive or behavioral relevance of these differences has largely been undetermined. We observe that the left SPL, a region of high individual variance at the cytoarchitectonic level, also demonstrates individual variance in its association with large scale resting-state networks and that network topology is linked to emotional intelligence. This topology-cognition relationship appears to be trans-diagnostic and is observed in both schizophrenia and healthy comparison populations. More generally, the implications of this result extend beyond imaging studies of social cognition. The demonstration that individual brain network topology is associated with individual variation in complex cognition reinforces a growing appreciation of the limitations of group-based averaging in resting-state imaging. Averaging across groups of subjects likely obfuscates relationships between individual network topology and cognitive and behavioral phenotypes. In this example, the relationship between network topology and cognitive measures was significant enough to be discerned in a group of a hundred subjects scanned a single time each. It seems inevitable that other relationships between network topology and cognition/behavior remain to be discovered but discerning those relationships may likely require "dense" scanning of individual subjects i.e. scanning the same individuals five (Mueller et al., 2013), twelve (Gordon et al., 2017b), or twenty-four times (Braga and Buckner, 2017). Such efforts are resource intensive, but if such deep characterization yields greater understanding of network-behavior relationships, it is reasonable to imagine a re-allocation of resources away from participant numbers and towards precise network mapping. A remaining challenge to be addressed is how such a change in approach may be applied to better understand the network basis of neurological and psychiatric disorders where acquiring multiple scans in symptomatic individuals may prove difficult.

## Funding sources

This work was supported by the National Institutes of Health: K23MH100623 (RB), RO1MH92440 (SE, MK), K24MH104449 (DO), K23MH091210 (KEL).

## Acknowledgements

We are grateful to the participants of this study and to anonymous reviewers for their suggestions during the peer review process.

## Appendix A. Supplementary data

Supplementary data to this article can be found online at https://doi.org/10.1016/j.neuroimage.2019.01.013.

## References

Abram, S.V., Wisner, K.M., Fox, J.M., Barch, D.M., Wang, L., Csernansky, J.G., MacDonald 3rd, A.W., Smith, M.J., 2017. Fronto-temporal connectivity predicts cognitive empathy deficits and experiential negative symptoms in schizophrenia. Hum. Brain Mapp. 38, 1111–1124.

Allen, D.N., Strauss, G.P., Donohue, B., van Kammen, D.P., 2007. Factor analytic support for social cognition as a separable cognitive domain in schizophrenia. Schizophr. Res. 93, 325–333.

Ashburner, J., 2007. A fast diffeomorphic image registration algorithm. Neuroimage 38, 95–113.

Baker, J.T., Holmes, A.J., Masters, G.A., Yeo, B.T., Krienen, F., Buckner, R.L., Ongur, D., 2014. Disruption of cortical association networks in schizophrenia and psychotic bipolar disorder. JAMA Psychiatry 71, 109–118.

Bijsterbosch, J.D., Woolrich, M.W., Glasser, M.F., Robinson, E.C., Beckmann, C.F., Van Essen, D.C., Harrison, S.J., Smith, S.M., 2018. The relationship between spatial configuration and functional connectivity of brain regions. Elife 7.

Bora, E., Yucel, M., Pantelis, C., 2009. Cognitive endophenotypes of bipolar disorder: a meta-analysis of neuropsychological deficits in euthymic patients and their first-degree relatives. J. Affect. Disord. 113, 1–20.

Braga, R.M., Buckner, R.L., 2017. Parallel interdigitated distributed networks within the individual estimated by intrinsic functional connectivity. Neuron 95, 457–471 e455.
Desikan, R.S., Segonne, F., Fischl, B., Quinn, B.T., Dickerson, B.C., Blacker, D., Buckner, R.L., Dale, A.M., Maguire, R.P., Hyman, B.T., Albert, M.S., Killiany, R.J., 2006. An automated labeling system for subdividing the human cerebral cortex on MRI scans into gyral based regions of interest. Neuroimage 31, 968–980.
Dodell-Feder, D., Delisi, L.E., Hooker, C.I., 2014. The relationship between default mode network connectivity and social functioning in individuals at familial high-risk for schizophrenia. Schizophr. Res. 156, 87–95.
Eack, S.M., Greeno, C.G., Pogue-Geile, M.F., Newhill, C.E., Hogarty, G.E., Keshavan, M.S., 2010. Assessing social-cognitive deficits in schizophrenia with the Mayer-Salovey-Caruso emotional intelligence test. Schizophr. Bull. 36, 370–380.
Fett, A.K., Viechtbauer, W., Dominguez, M.D., Penn, D.L., van Os, J., Krabbendam, L., 2011. The relationship between neurocognition and social cognition with functional outcomes in schizophrenia: a meta-analysis. Neurosci. Biobehav. Rev. 35, 573–588.
Finn, E.S., Shen, X., Scheinost, D., Rosenberg, M.D., Huang, J., Chun, M.M., Papademetris, X., Constable, R.T., 2015. Functional connectome fingerprinting: identifying individuals using patterns of brain connectivity. Nat. Neurosci. 18, 1664–1671.
First, M.B., 1998. Structured Clinical Interview for DSM-IV Axis I Disorders: Patient Edition (February 1996 Final), SCID-I/P. Biometrics Research Department, New York State Psychiatric Institute.
First, M.B., New York State Psychiatric Institute Biometrics Research, D., 2007. Structured Clinical Interview for DSM-IV-TR axis I Disorders : SCID-I. Biometrics Research Dept., New York State Psychiatric Institutute, New York, N.Y.
Fox, J.M., Abram, S.V., Reilly, J.L., Eack, S., Goldman, M.B., Csernansky, J.G., Wang, L., Smith, M.J., 2017. Default mode functional connectivity is associated with social functioning in schizophrenia. J. Abnorm. Psychol. 126, 392–405.
Fox, M.D., Snyder, A.Z., Vincent, J.L., Corbetta, M., Van Essen, D.C., Raichle, M.E., 2005. The human brain is intrinsically organized into dynamic, anticorrelated functional networks. Proc. Natl. Acad. Sci. U. S. A. 102, 9673–9678.
Friston, K.J., Williams, S., Howard, R., Frackowiak, R.S., Turner, R., 1996. Movement-related effects in fMRI time-series. Magn. Reson. Med. 35, 346–355.
Gordon, E.M., Laumann, T.O., Adeyemo, B., Gilmore, A.W., Nelson, S.M., Dosenbach, N.U.F., Petersen, S.E., 2017a. Individual-specific features of brain systems identified with resting state functional correlations. Neuroimage 146, 918–939.
Gordon, E.M., Laumann, T.O., Gilmore, A.W., Newbold, D.J., Greene, D.J., Berg, J.J., Ortega, M., Hoyt-Drazen, C., Gratton, C., Sun, H., Hampton, J.M., Coalson, R.S., Nguyen, A.L., McDermott, K.B., Shimony, J.S., Snyder, A.Z., Schlaggar, B.L., Petersen, S.E., Nelson, S.M., Dosenbach, N.U.F., 2017b. Precision functional mapping of individual human brains. Neuron 95, 791–807 e797.
Green, M.F., 2016. Impact of cognitive and social cognitive impairment on functional outcomes in patients with schizophrenia. J. Clin. Psychiatr. 77 (Suppl. 2), 8–11.
Green, M.F., Horan, W.P., Lee, J., 2015. Social cognition in schizophrenia. Nat. Rev. Neurosci. 16, 620–631.
Green, M.F., Penn, D.L., Bentall, R., Carpenter, W.T., Gaebel, W., Gur, R.C., Kring, A.M., Park, S., Silverstein, S.M., Heinssen, R., 2008. Social cognition in schizophrenia: an NIMH workshop on definitions, assessment, and research opportunities. Schizophr. Bull. 34, 1211–1220.
Hays, J.R., Reas, D.L., Shaw, J.B., 2002. Concurrent validity of the Wechsler abbreviated scale of intelligence and the Kaufman brief intelligence test among psychiatric inpatients. Psychol. Rep. 90, 355–359.
Hoe, M., Nakagami, E., Green, M.F., Brekke, J.S., 2012. The causal relationships between neurocognition, social cognition and functional outcome over time in schizophrenia: a latent difference score approach. Psychol. Med. 42, 2287–2299.
Jenkinson, M., Beckmann, C.F., Behrens, T.E., Woolrich, M.W., Smith, S.M., 2012. Fsl. Neuroimage 62, 782–790.
Jung, R.E., Haier, R.J., 2007. The Parieto-Frontal Integration Theory (P-FIT) of intelligence: converging neuroimaging evidence. Behav. Brain Sci. 30, 135–154 discussion 154-187.
Kim, S., 2015. Ppcor: an R package for a fast calculation to semi-partial correlation coefficients. Commun Stat Appl Methods 22, 665–674.
Kohler, C.G., Walker, J.B., Martin, E.A., Healey, K.M., Moberg, P.J., 2010. Facial emotion perception in schizophrenia: a meta-analytic review. Schizophr. Bull. 36, 1009–1019.
Laumann, T.O., Gordon, E.M., Adeyemo, B., Snyder, A.Z., Joo, S.J., Chen, M.Y., Gilmore, A.W., McDermott, K.B., Nelson, S.M., Dosenbach, N.U., Schlaggar, B.L., Mumford, J.A., Poldrack, R.A., Petersen, S.E., 2015. Functional system and areal organization of a highly sampled individual human brain. Neuron 87, 657–670.
Lewandowski, K.E., Ongur, D., Keshavan, M.S., 2018. Development of novel behavioral interventions in an experimental therapeutics world: challenges, and directions for the future. Schizophr. Res. 192, 6–8.
Marder, S.R., 2006. The NIMH-MATRICS project for developing cognition-enhancing agents for schizophrenia. Dialogues Clin. Neurosci. 8, 109–113.
Mars, R.B., Jbabdi, S., Sallet, J., O'Reilly, J.X., Croxson, P.L., Olivier, E., Noonan, M.P., Bergmann, C., Mitchell, A.S., Baxter, M.G., Behrens, T.E., Johansen-Berg, H., Tomassini, V., Miller, K.L., Rushworth, M.F., 2011. Diffusion-weighted imaging tractography-based parcellation of the human parietal cortex and comparison with human and macaque resting-state functional connectivity. J. Neurosci. 31, 4087–4100.
Mars, R.B., Neubert, F.X., Noonan, M.P., Sallet, J., Toni, I., Rushworth, M.F., 2012. On the relationship between the "default mode network" and the "social brain". Front. Hum. Neurosci. 6, 189.
Mayer, J.D., Salovey, P., Caruso, D.R., Sitarenios, G., 2003. Measuring emotional intelligence with the MSCEIT V2.0. Emotion 3, 97–105.
Mehta, U.M., Bhagyavathi, H.D., Thirthalli, J., Kumar, K.J., Gangadhar, B.N., 2014. Neurocognitive predictors of social cognition in remitted schizophrenia. Psychiatr. Res. 219, 268–274.
Mehta, U.M., Thirthalli, J., Subbakrishna, D.K., Gangadhar, B.N., Eack, S.M., Keshavan, M.S., 2013. Social and neuro-cognition as distinct cognitive factors in schizophrenia: a systematic review. Schizophr. Res. 148, 3–11.
Mueller, S., Wang, D., Fox, M.D., Yeo, B.T., Sepulcre, J., Sabuncu, M.R., Shafee, R., Lu, J., Liu, H., 2013. Individual variability in functional connectivity architecture of the human brain. Neuron 77, 586–595.
Nuechterlein, K.H., Green, M.F., Kern, R.S., Baade, L.E., Barch, D.M., Cohen, J.D., Essock, S., Fenton, W.S., Frese 3rd, F.J., Gold, J.M., Goldberg, T., Heaton, R.K., Keefe, R.S., Kraemer, H., Mesholam-Gately, R., Seidman, L.J., Stover, E., Weinberger, D.R., Young, A.S., Zalcman, S., Marder, S.R., 2008. The MATRICS Consensus Cognitive Battery, part 1: test selection, reliability, and validity. Am. J. Psychiatry 165, 203–213.
Pisner, D.A., Smith, R., Alkozei, A., Klimova, A., Killgore, W.D., 2017. Highways of the emotional intellect: white matter microstructural correlates of an ability-based measure of emotional intelligence. Soc. Neurosci. 12, 253–267.
Poldrack, R.A., Laumann, T.O., Koyejo, O., Gregory, B., Hover, A., Chen, M.Y., Gorgolewski, K.J., Luci, J., Joo, S.J., Boyd, R.L., Hunicke-Smith, S., Simpson, Z.B., Caven, T., Sochat, V., Shine, J.M., Gordon, E., Snyder, A.Z., Adeyemo, B., Petersen, S.E., Glahn, D.C., Reese Mckay, D., Curran, J.E., Goring, H.H., Carless, M.A., Blangero, J., Dougherty, R., Leemans, A., Handwerker, D.A., Frick, L., Marcotte, E.M., Mumford, J.A., 2015. Long-term neural and physiological phenotyping of a single human. Nat. Commun. 6, 8885.
Power, J.D., Barnes, K.A., Snyder, A.Z., Schlaggar, B.L., Petersen, S.E., 2012. Spurious but systematic correlations in functional connectivity MRI networks arise from subject motion. Neuroimage 59, 2142–2154.
Power, J.D., Cohen, A.L., Nelson, S.M., Wig, G.S., Barnes, K.A., Church, J.A., Vogel, A.C., Laumann, T.O., Miezin, F.M., Schlaggar, B.L., Petersen, S.E., 2011. Functional network organization of the human brain. Neuron 72, 665–678.
Rosenberg, M.D., Finn, E.S., Scheinost, D., Papademetris, X., Shen, X., Constable, R.T., Chun, M.M., 2016. A neuromarker of sustained attention from whole-brain functional connectivity. Nat. Neurosci. 19, 165–171.
Salovey, Mayer, 1990. Emotional intelligence. Imagin., Cognit. Pers. 9, 185–211.
Satterthwaite, T.D., Vandekar, S.N., Wolf, D.H., Bassett, D.S., Ruparel, K., Shehzad, Z., Craddock, R.C., Shinohara, R.T., Moore, T.M., Gennatas, E.D., Jackson, C., Roalf, D.R., Milham, M.P., Calkins, M.E., Hakonarson, H., Gur, R.C., Gur, R.E., 2015. Connectome-wide network analysis of youth with Psychosis-Spectrum symptoms. Mol. Psychiatr. 20, 1508–1515.
Savla, G.N., Vella, L., Armstrong, C.C., Penn, D.L., Twamley, E.W., 2013. Deficits in domains of social cognition in schizophrenia: a meta-analysis of the empirical evidence. Schizophr. Bull. 39, 979–992.
Scheperjans, F., Eickhoff, S.B., Homke, L., Mohlberg, H., Hermann, K., Amunts, K., Zilles, K., 2008. Probabilistic maps, morphometry, and variability of cytoarchitectonic areas in the human superior parietal cortex. Cerebr. Cortex 18, 2141–2157.
Sergi, M.J., Rassovsky, Y., Widmark, C., Reist, C., Erhart, S., Braff, D.L., Marder, S.R., Green, M.F., 2007. Social cognition in schizophrenia: relationships with neurocognition and negative symptoms. Schizophr. Res. 90, 316–324.
Shanmugan, S., Wolf, D.H., Calkins, M.E., Moore, T.M., Ruparel, K., Hopson, R.D., Vandekar, S.N., Roalf, D.R., Elliott, M.A., Jackson, C., Gennatas, E.D., Leibenluft, E., Pine, D.S., Shinohara, R.T., Hakonarson, H., Gur, R.C., Gur, R.E., Satterthwaite, T.D., 2016. Common and dissociable mechanisms of executive system dysfunction across psychiatric disorders in youth. Am. J. Psychiatry 173, 517–526.
Sharma, A., Wolf, D.H., Ciric, R., Kable, J.W., Moore, T.M., Vandekar, S.N., Katchmar, N., Daldal, A., Ruparel, K., Davatzikos, C., Elliott, M.A., Calkins, M.E., Shinohara, R.T., Bassett, D.S., Satterthwaite, T.D., 2017. Common dimensional reward deficits across mood and psychotic disorders: a connectome-wide association study. Am. J. Psychiatry 174, 657–666 appiajp201616070774.
Shehzad, Z., Kelly, C., Reiss, P.T., Cameron Craddock, R., Emerson, J.W., McMahon, K., Copland, D.A., Castellanos, F.X., Milham, M.P., 2014. A multivariate distance-based analytic framework for connectome-wide association studies. Neuroimage 93 (Pt 1), 74–94.
Smith, S.M., Nichols, T.E., Vidaurre, D., Winkler, A.M., Behrens, T.E., Glasser, M.F., Ugurbil, K., Barch, D.M., Van Essen, D.C., Miller, K.L., 2015. A positive-negative mode of population covariation links brain connectivity, demographics and behavior. Nat. Neurosci. 18, 1565–1567.
Sprong, M., Schothorst, P., Vos, E., Hox, J., van Engeland, H., 2007. Theory of mind in schizophrenia: meta-analysis. Br. J. Psychiatry 191, 5–13.
Van Essen, D.C., Drury, H.A., Dickson, J., Harwell, J., Hanlon, D., Anderson, C.H., 2001. An integrated software suite for surface-based analyses of cerebral cortex. J. Am. Med. Inf. Assoc. 8, 443–459.
Wang, D., Buckner, R.L., Fox, M.D., Holt, D.J., Holmes, A.J., Stoecklein, S., Langs, G., Pan, R., Qian, T., Li, K., Baker, J.T., Stufflebeam, S.M., Wang, K., Wang, X., Hong, B., Liu, H., 2015a. Parcellating cortical functional networks in individuals. Nat. Neurosci. 18, 1853–1860.
Wang, J., Yang, Y., Fan, L., Xu, J., Li, C., Liu, Y., Fox, P.T., Eickhoff, S.B., Yu, C., Jiang, T., 2015b. Convergent functional architecture of the superior parietal lobule unraveled with multimodal neuroimaging approaches. Hum. Brain Mapp. 36, 238–257.
Yan, C.G., Cheung, B., Kelly, C., Colcombe, S., Craddock, R.C., Di Martino, A., Li, Q., Zuo, X.N., Castellanos, F.X., Milham, M.P., 2013. A comprehensive assessment of regional variation in the impact of head micromovements on functional connectomics. Neuroimage 76, 183–201.
Yan, C.G., Wang, X.D., Zuo, X.N., Zang, Y.F., 2016. DPABI: data processing & analysis for (Resting-State) brain imaging. Neuroinformatics 14, 339–351.

Yang, G.J., Murray, J.D., Wang, X.J., Glahn, D.C., Pearlson, G.D., Repovs, G., Krystal, J.H., Anticevic, A., 2016. Functional hierarchy underlies preferential connectivity disturbances in schizophrenia. Proc. Natl. Acad. Sci. U. S. A. 113, E219–E228.
Yeo, B.T., Krienen, F.M., Sepulcre, J., Sabuncu, M.R., Lashkari, D., Hollinshead, M., Roffman, J.L., Smoller, J.W., Zollei, L., Polimeni, J.R., Fischl, B., Liu, H., Buckner, R.L., 2011. The organization of the human cerebral cortex estimated by intrinsic functional connectivity. J. Neurophysiol. 106, 1125–1165.
Zapala, M.A., Schork, N.J., 2006. Multivariate regression analysis of distance matrices for testing associations between gene expression patterns and related variables. Proc. Natl. Acad. Sci. U. S. A. 103, 19430–19435.